Correlated neutrino and photon emission from Mrk 421 during flares

Maria Petropoulou, Purdue University, West Lafayette, 47907 IN, USA
Stefan Coenders, Technische Universität München, D-85748 Garching, Germany
Stavros Dimitrakoudis, University of Alberta, Edmonton, Canada

Abstract

Blazars, being highly variable sources across the electromagnetic spectrum, may serve as promising targets for high-energy neutrino detection, especially during periods of flaring activity. Using the nearby blazar Mrk 421 as a testbed, we present a detailed hadronic model of its emission during a 13-day flaring period. We calculate the expected muon neutrino event rate observed by IceCube at energies > 1 PeV, and compare it with that expected from a longer, yet non-flaring, period of emission. After applying the derived correlation between the > 1 PeV neutrino and 0.1-300 GeV emission to the long-term *Fermi*-LAT light curve of Mrk 421, we calculate the expected number of muon neutrino events above 1 PeV within 5 years of full IceCube detector livetime and discuss the implications of the results.

1 Introduction

Ground-based imaging Cherenkov observatories, such as H.E.S.S. [1], MAGIC [2] and VERITAS [3], in synergy with the *Fermi*-Large Area Telescope (LAT) [4], have accumulated sufficient γ-ray data to convincingly prove that blazars, a class of active galactic nuclei (AGN) whose jets point along our line of sight, are efficient particle accelerators. It is commonly accepted that particle acceleration takes place in an "active" region of the blazar jet; this could be a standing shock wave [5, 6] or sites of relativistic magnetic reconnection [7, 8, 9].

Irrespectively of the specifics of the particle acceleration process, both electrons and protons are expected to achieve relativistic energies. In principle, protons reach higher energies than electrons, since they are less affected by energy loss processes at the acceleration site. It is a therefore a natural assumption that both leptonic and hadronic emission processes will contribute, to a certain degree, to the production of the multi-wavelength (MW) blazar emission. In a nutshell, in such scenarios the characteristic blazar spectral energy distribution (SED) that shows two humps in a νL_ν vs. ν diagram [10, 11] is explained in terms of electron synchrotron radiation (from radio up to UV/X-rays) and of hadronic-related processes (from MeV to TeV γ-rays). The latter include proton synchrotron radiation [12, 13], pion-related cascades [14, 15] and synchrotron radiation of pion-produced pairs [16, 17]. Besides their imprint on the blazar SED, the ultimate proof for the presence of relativistic protons in blazar jets can come only from the detection of high-energy neutrinos (e.g. [18, 19]).

Blazars are intrinsically variable sources, especially at the X-ray and γ-ray regime. It is therefore evident that the assumption of a constant photon flux, entering in many model-independent calculations of the blazar neutrino emission, is an oversimplification. An accurate modeling of the neutrino emission in both quiescent and flaring states of blazar emission, which acts complementary to model-independent studies (e.g. [20, 21]), is vital for the interpretation of observations by neutrino telescopes, especially in the context of the discovery of astrophysical neutrino events with energies > 100 TeV by IceCube [22, 23].

2 Aims

The blazar Mrk 421 is one of the nearest ($z = 0.031$) and brightest BL Lac sources in the extragalactic X-ray sky and very high energy (VHE; $E_\gamma > 100$ GeV) sky [24], which makes it an ideal target of MW observing campaigns (see also Fig. 1). The 2009 MW campaign [25] covered approximately a four-month long non-flaring period, which is a good representation of the blazar's quiescent emission. The respective neutrino emission has been calculated and presented in [16]. Here, we expand upon the work of [16] by studying the neutrino emission from Mrk 421 during a flaring period in both X- and γ-ray energy bands. To this end, we apply our model to the 13-day flare of 2010 (MJD 55265-55277), having an unprecedented MW (from radio up to TeV γ-rays) and simultaneous (within 2-3 hours) coverage [26]. With this study we aim to:

1. test the applicability of the model to an active state of blazar emission;
2. calculate the temporal evolution of the neutrino spectrum during a flaring period of a blazar and calculate the respective neutrino light curve;
3. test possible correlations between the neutrino and photon fluxes in different energy bands (e.g. X-rays and γ-rays);
4. calculate the neutrino flux from Mrk 421 during a γ-ray flare and compare it against the one expected from a longer, but non-flaring period, i.e. in quiescence;
5. make predictions about the cumulative number of neutrino events that IceCube should detect in t years, after applying the photon-neutrino flux correlations, if any, to the long-term γ-ray (*Fermi*-LAT) light curve of Mrk 421.

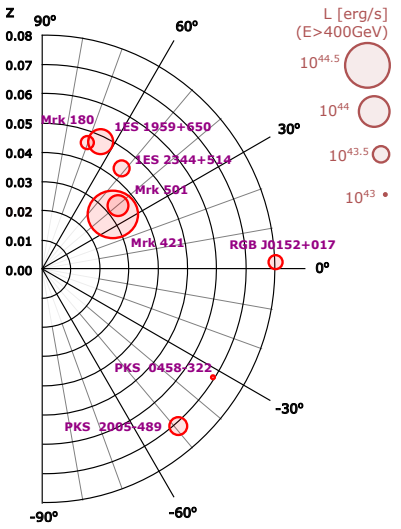

Figure 1: Polar diagram of the closest ($z < 0.1$) TeV-selected blazars to Earth that have also been observed at high-energies (HE; 0.1 GeV$< E_\gamma <$ 300 GeV) with *Fermi*-LAT. The size of the circles indicates their apparent γ-ray luminosity above 400 GeV. All data are adopted from [24].

By investigating the aforementioned issues, we plan to address the more general question of whether γ-ray flares determine the optimum time window for high-energy neutrino detection from the nearby blazar Mrk 421.

3 Theoretical framework and IceCube analysis

3.1 Theoretical model

Here, we summarize the basic features of the adopted theoretical models. A detailed description can be found in [27, 16]. We assume that the region responsible for the blazar emission can be described as a spherical blob of radius r'_b, containing a tangled magnetic field of strength B' and moving with a Doppler factor δ_D. Relativistic protons and (primary) electrons with a power-law distribution in energies are injected isotropically in the volume of the blob with a constant luminosity, while they may escape on a characteristic timescale r'_b/c. Pion ($\pi^\pm, \pi^0$) production is a natural outcome of photohadronic interactions between the relativistic protons and the internal photons, which are predominantly synchrotron photons emitted by the primary electrons. The decay of charged pions results in the injection of secondary relativistic electrons and positrons ($\pi^\pm \to \mu^\pm + \nu_\mu(\bar{\nu}_\mu)$, $\mu^\pm \to e^\pm + \bar{\nu}_\mu(\nu_\mu) + \nu_{\rm e}(\bar{\nu}_{\rm e})$), whose synchrotron emission may emerge in the γ-ray regime. Neutral pions decay into VHE γ-rays (e.g. $E_\gamma \sim 10$ PeV, for a parent proton with energy $E_{\rm p} = 100$ PeV), and those are, in turn, susceptible to $\gamma\gamma$ absorption and can initiate an electromagnetic (or hadronic)

cascade [14, 15]. Protons may also interact with photons, producing e^-e^+ pairs through the Bethe-Heitler process (see also [28]). As synchrotron self-Compton (SSC) emission from primary electrons may also emerge in the γ-ray energy band, the observed γ-ray emission can be totally or partially explained by photohadronic processes, depending on the specifics of individual sources [29]. We remark that photopion production is the only process that is relevant to blazar jets, for the purposes of high-energy neutrino emission.

The interplay of the processes governing the evolution of the five stable particle populations is formulated with a set of five time-dependent, energy-conserving kinetic equations. To simultaneously solve the coupled kinetic equations for all particle types we use the time-dependent code described in [30].

3.2 Neutrino point source searches with IceCube

The high-energy starting event (HESE) analysis consists of a small, albeit high-purity, statistical sample of astrophysical neutrinos due to the imposed veto on atmospheric events. The high purity comes at the cost of a significantly reduced effective area. Although the HESE sample is composed of neutrinos of all flavours, only the the muon track events can actually yield a true identification of a neutrino point source, thanks to their good angular resolution. Thus, the neutrino event rates presented here were calculated using the typical IceCube up-going muon samples, similar to those in [31, 32]. The reasons are summarized below:

- in the northern sky, where Mrk 421 is located, muons are shielded by the Earth and the event selection yields a clear sample of astrophysical neutrinos down to ~ 100 TeV energies;
- the background of irreducible atmospheric neutrinos is not an issue as it is limited to small amounts due to the very good angular resolution of track-like events ($< 1^\circ$). The latter is important as it reduces the possible background of diffuse astrophysical neutrinos a lot compared to cascade-like events that have large uncertainties of $\sim 10^\circ$;
- the available effective volume for neutrino interactions in the analysis of up-going muons exceeds that of the HESE analysis by a factor of ~ 50.

4 Results and Interpretation

In Fig. 2 (left panel) we present an indicative fit to the SED of Mrk 421 on the first day of the 13-day flare (MJD 55265) in 2010 (black solid line). This is compared to the model SED of the four-month long quiescent period of 2009 (grey line). In both cases, the leptohadronic model can successfully explain the MW emission of Mrk 421. The daily all-flavour neutrino spectra as derived after modelling the SEDs for 13 consecutive days are presented in the right panel of Fig. 2. It becomes evident that the > 1 PeV neutrino flux correlates with the photon flux in the X-ray, HE and VHE γ-ray energy bands. In particular, $\log F_\nu = A \log F_\gamma + B$, where F_γ is defined as the γ-ray flux in the 0.1-300 GeV energy band, $A = 1.59 \pm 0.17$ and $B = 5.25 \pm 1.64$. In contrast, the sub-PeV neutrino flux in our model is not correlated with any of the aforementioned photon fluxes. Using the analysis described in §3.2 we calculated the expected IceCube neutrino event rate for the $\nu_\mu + \bar{\nu}_\mu$ daily SEDs shown in Fig. 2 compared to the background event count rate (see Table 1). Interestingly, the $\nu_\mu + \bar{\nu}_\mu$ event rate for $E_\nu > 100$ TeV as obtained from the 13-day flare and the 4-month long quiescent period is ~ 0.57 evt/yr. This translates to $\sim 0.57 \times 13/333 \sim 0.02$ expected events for the 13-day flare and $\sim 0.57 \times 120/333 \sim 0.2$ events for the quiescent period of 2009. *Thus, an accumulation of many flares similar to that of 2010 is needed in order to detect neutrinos from Mrk 421 with IceCube. In this light, caution is needed when associating a ν event with a flaring blazar lying in the error circle of the neutrino detection.*

Assuming that the correlation is present over longer time periods as well, we may apply the derived linear relation between $\log F_\nu$ and $\log F_\gamma$ to the long-term light curve at a specific energy band, in order to calculate the expected number of muon neutrino events at $E_\nu \geq 1$ PeV within the five years of full IceCube detector livetime. Our calculations, thus, take into account the γ-ray variability of the

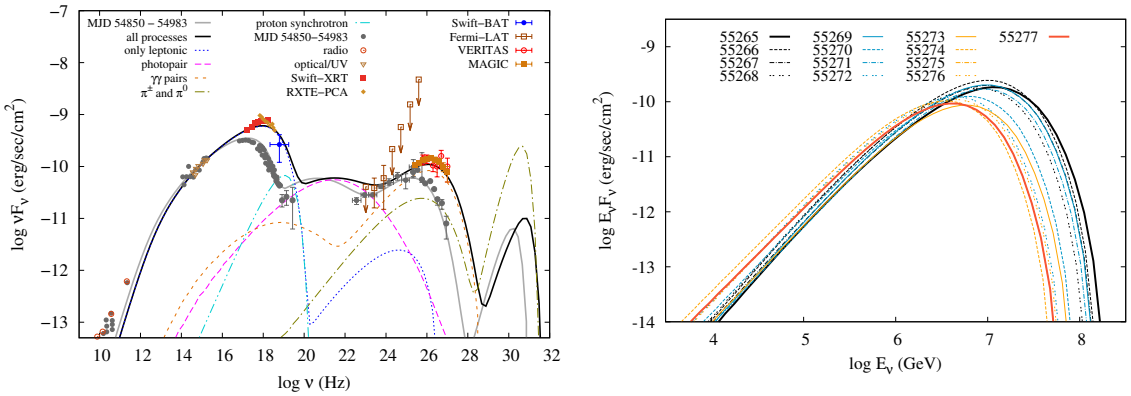

Figure 2: **Left panel**: Simultaneous multi-wavelength SED of Mrk 421 on MJD 55265. Different symbols denote the various instruments used to collect the data, and their meaning is given in the legends. All data-points are from [26]. The grey circles depict the time-averaged SED of Mrk 421 over the period MJD 54850-54983 [25]. This is a good representation of the blazar non-flaring (quiescent) emission. The model-derived spectra that fit the daily SEDs are plotted with black thick lines. The grey thick lines are a fit to the quiescent emission. Different types of lines are used to present the spectra from different emission processes: proton synchrotron radiation (light blue dashed double-dotted line), (primary) electron synchrotron and SSC emission (blue dotted line), synchrotron radiation from Bethe-Heitler pairs (magenta long-dashed line), synchrotron radiation of pairs from $\pi^{\pm}, \mu^{\pm}$ decays and γ-rays from π^0 decays (gold dashed-dotted line), synchrotron radiation of pairs from $\gamma\gamma$ absorption (orange short-dashed line). **Right panel**: All-flavour neutrino ($\nu + \bar{\nu}$) fluxes derived by the model for the period MJD 55265-55277.

blazar by employing the model-predicted correlations. Interestingly, after 2012 the source exhibited four flares with month-long durations and peak fluxes 3-10 higher than that of the 13-day flare in 2010. Henceforth, we will refer to them as "major flares".

We calculated N_ν for the following three cases: (i) we performed the analysis using the full *Fermi*-LAT light curve ('w flares' analysis); (ii) we performed the analysis after excluding the major flares ('w/o flares' analysis) in order to exemplify the net effect of the major flares on the expected number of muon neutrino events; and (iii) we considered the extreme case of a non-variable γ-ray light curve with flux equal to that of the 2009 quiescent period ('quiescent' analysis). The latter can be directly applied to neutrinos with 100 TeV$< E_\nu <$1 PeV (see also right panel in Fig. 2). Our results are presented in Table 2 and Fig. 3. The meaning of different curves is explained in the figure caption.

Fig. 3 and Table 2 indicate that the predictions for the cumulative event count above 1 PeV are significantly affected by the major flares under the assumption of a neutrino-γ-ray flux correlation. In

Table 1: Expected IceCube neutrino event rate for the $\nu_\mu + \bar{\nu}_\mu$ daily SEDs shown in Fig. 2 compared to the background event count rate. For the point spread function, a 90% angular resolution of 1° was assumed. All neutrino event rates are in units of yr^{-1} assuming a good IceCube runtime of ~ 333 days per year, same as for the most recent point source data [31].

	Mrk 421[a]		Background[b]	
E_ν (TeV)	13-day flare (55265-55277)	quiescent (54850-54983)	atmospheric	diffuse
$0.1 - 100$	0.023	0.019	7.371	0.010
$100 - 10^3$	0.264	0.282	1.852×10^{-3}	2.203×10^{-3}
$10^3 - 5 \times 10^4$	0.306	0.288	4.554×10^{-6}	2.236×10^{-4}

[a] 90% of the signal flux is expected to be within $\Delta\Psi < 1°$.
[b] Integrated over the bin-size $\Delta\Psi < 1°$.

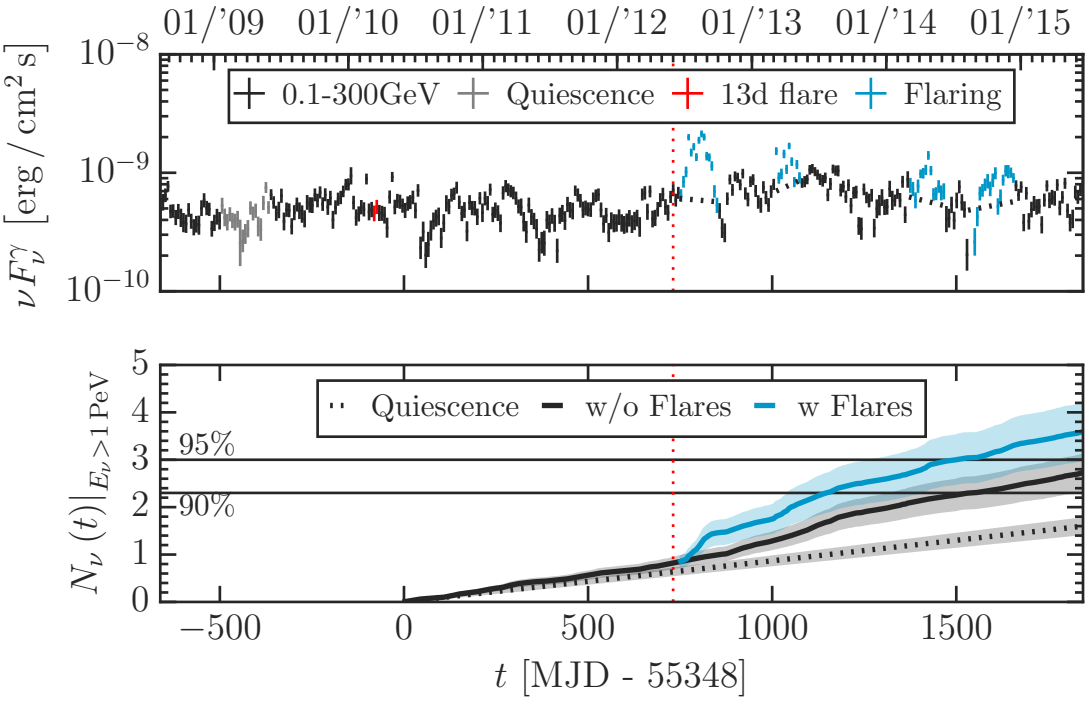

Figure 3: **Top panel**: Long-term, weekly binned γ-ray light curve of Mrk 421 at 0.1-300 GeV as observed with *Fermi*-LAT. The quiescent period and the 13-day flare are highlighted with grey and red symbols, respectively. At least four major flares (for the definition, see text) can be identified (light blue symbols). **Bottom panel**: The cumulative number of muon neutrino events above 1 PeV expected for IceCube within time t. The calculation is performed using the $\nu_\mu + \bar{\nu}_\mu$ flux estimated by the γ-ray light curve (top panel). The $\nu_\mu + \bar{\nu}_\mu$ flux is assumed to correlate with the *Fermi*-LATγ-ray flux as $F_{\nu_\mu} \propto (F_\gamma)^A$, where $A = 1.59 \pm 0.17$. The cumulative curves obtained with and without the major flares included in the analysis are plotted with thick light blue ('w flares') and black ('w/o flares') lines, respectively. The results of the 'quiescent analysis', where a constant γ-ray flux, equal to that of the quiescent period (grey points in top panel) is assumed, are plotted with a dotted line. These correspond also to the expected N_ν for 100 TeV $< E_\nu <$ 1 PeV. In all cases, the 90% uncertainties on the mean expected count are shown as shaded bands. These take into account the systematic uncertainties of the IceCube effective area, the statistical uncertainties of the γ-ray observations, and the error of the slope in the relation $\log F_\nu - \log F_\gamma$. Horizontal lines indicate the threshold for the observation of one or more neutrinos at 90% or 95% CL. The latest published results of IceCube [31] included data until MJD 56063, which is marked by the vertical red-dotted line.

Table 2: Number of high-energy $\nu_\mu + \bar{\nu}_\mu$ events ($E_\nu > 1$ PeV) expected for IceCube in various seasons of operation (each with duration T in days). The results are obtained using the *Fermi*-LAT γ-ray light curve in Fig. 3 (top panel) and the correlation with the high-energy neutrino flux. The values for each season are obtained after replacing the major γ-ray flares (Table 2) with a non-variable emission, whose flux was determined through interpolation of the γ-ray light curve just before the start and after the end of each major flare (for details, see text). The total number of events without (with) the major flares included are also presented. For each entry, the probability $P_{N_\nu \geq 1}$ of observing one or more neutrinos is quoted.

Season	T (days)	$\nu_\mu + \bar{\nu}_\mu$	$P_{N_\nu \geq 1}(\%)^\dagger$
06/2010-05/2011	364	0.43 ± 0.06	34 ± 4
06/2011-05/2012	364	0.38 ± 0.05	32 ± 3
06/2012-05/2013	371	0.71 ± 0.11	51 ± 5
06/2013-05/2014	364	0.70 ± 0.11	50 ± 5
06/2014-05/2015	350	0.47 ± 0.06	38 ± 4
$\sum$ w/o Flares	1834[a]	2.73 ± 0.38	94 ± 2
$\sum$ w Flares	1834	3.59 ± 0.60	97 ± 2

† Using Poisson statistics, $P(N_\nu \geq 1) = 1 - \mathrm{e}^{-\lambda}$ for a Poisson distribution with mean λ.

[a] On top of the quoted years, three weeks of additional *Fermi*-LAT data are available after 05/2015.

Table 3: Same as Table 2 but for the four flares that were identified in this analysis.

No.	T (days)	$\nu_\mu + \bar{\nu}_\mu$	$P_{N_\nu \geq 1}(\%)$
Flares 1a+1b	105	0.61 ± 0.16	46 ± 8
Flare 2	70	0.32 ± 0.07	27 ± 5
Flare 3	98	0.26 ± 0.05	23 ± 4
Flares 4a+4b	112	0.26 ± 0.05	23 ± 4
$\sum$ Flares	385	1.46 ± 0.32	77 ± 7

particular, we find that 1.46 ± 0.32 $\nu_\mu + \bar{\nu}_\mu$ events are expected within a period of 385 days due to the four major flares. Thus, their presence increases the neutrino event rate within the IceCube livetime by 30% (see Tables 2 and 3). One should note though that none of the major flares alone could result to a neutrino detection (e.g. 0.61 ± 0.16 $\nu_\mu + \bar{\nu}_\mu$ events are expected from the extreme flare of 2012).

References

[1] J. A. Hinton and the HESS Collaboration, *NewAR* **48**, 331 (2004).

[2] E. Lorenz and The MAGIC Collaboration, *NewAR* **48**, 339 (2004).

[3] J. Holder et al., *AIPC* **1085**, 657 (2008).

[4] W. B. Atwood et al., *ApJ* **697**, 1071 (2009).

[5] A. P. Marscher and W. K. Gear, *ApJ* **298**, 114 (1985).

[6] D. Kazanas and D. C. Ellison, *ApJ* **304**, 178 (1986).

[7] D. Giannios, *MNRAS* **408**, 46 (2010).

[8] L. Sironi and A. Spitkovski, *ApJL* **783**, 21 (2014).

[9] L. Sironi, M. Petropoulou and D. Giannios, *MNRAS* **450**, 183 (2015).

[10] C. M. Urry and P. Padovani, *ARAA* **35**, 445 (1995).

[11] G. Fossati et al., *MNRAS* **299**, 443 (1998).

[12] F. A. Aharonian, *NewA* **5**, 377 (2000).

[13] A. Mücke and R. J. Protheroe, *APh* **15**, 21 (2001).

[14] K. Mannheim, P. L. Biermann and W. M. Kruells, *A&A* **251**, 723 (1991).

[15] K. Mannheim and P. L. Biermann, *A&A* **253**, 21 (1992).

[16] S. Dimitrakoudis, M. Petropoulou and A. Mastichiadis *APh* **54**, 61 (2014).

[17] M. Cerruti et al., *MNRAS* **448**, 910 (2015).

[18] F. W. Stecker et al., *PhRvL* **66**, 2697 (1991).

[19] F. Halzen and E. Zas, *ApJ* **488**, 669 (1997).

[20] M. Doert et al., *JPhCS* **355**, 012039 (2012).

[21] N. Fraija and A. Marinelli, *APh* **70**, 54 (2015).

[22] IceCube Collaboration, *Science* **342** (2013).

[23] M. G. Aartsen et al., *PhRvL* **113**, 10 (2014).

[24] G. D. Şentürk et al., *ApJ* **764**, 119 (2013).

[25] A. A. Abdo et al., *ApJ* **736**, 131 (2011).

[26] Aleksić, J. et al., *A&A* **578**, A22 (2015).

[27] A. Mastichiadis, M. Petropoulou and S. Dimitrakoudis *MNRAS* **434**, 2684 (2013).

[28] M. Petropoulou and A. Mastichiadis, *MNRAS* **447**, 36 (2015).

[29] M. Petropoulou et al., *MNRAS* **448**, 2412 (2015).

[30] S. Dimitrakoudis et al., *A&A* **546**, A120 (2012).

[31] M. G. Aartsen et al., *ApJ* **796**, 109 (2014).

[32] M. G. Aartsen et al., *PhRvL* **115**, 8 (2015).